

From aggregation to inhibition: N-amination converts amyloidogenic tau peptides into soluble antagonists of cellular seeding

Kamlesh M. Makwana[†], Matthew P. Sarnowski[†], Jiayuan Miao[‡], Yu-Shan Lin[‡], and Juan R. Del Valle^{†*}

[†]Department of Chemistry & Biochemistry, University of Notre Dame, Notre Dame, IN 46556, United States

[‡]Department of Chemistry, Tufts University, Medford, MA 02155, United States

KEYWORDS: Amyloid, protein-protein interaction, peptidomimetics, β -sheet, β -strand, tau, aggregation

ABSTRACT: The spread of neurofibrillary tangles resulting from tau protein aggregation is a hallmark of Alzheimer's and related neurodegenerative diseases. Early oligomerization of tau involves conformational reorganization into parallel β -sheet structures and supramolecular assembly into toxic fibrils. Despite the need for selective inhibitors of tau propagation, β -rich protein assemblies are inherently difficult to target with small molecules. Here, we describe a minimalist approach to mimic the aggregation-prone modules within tau. We carried out a backbone residue scan and show that amide N-amination completely abolishes the tendency of these peptides to self-aggregate, rendering them soluble mimics of ordered β -strands from the tau R2 and R3 domains. Several N-amino peptides (NAPs) inhibit disease-associated tau aggregation and prevent fibril formation *in vitro*. We further demonstrate that NAPs **12** and **13** are effective at blocking the cellular seeding of endogenous tau by interacting with both monomeric or fibrillar forms of extracellular tau. Peptidomimetic **12** is serum stable, non-toxic to neuronal cells, and selectively inhibits the aggregation of tau over A β ₄₂. Structural analysis of our lead NAPs shows considerable conformational constraint imposed by the N-amino groups. The enhanced rigidity and full complement of sidechains thus enables NAPs to recognize tau fibrils. The described backbone N-amination approach provides a rational basis for the mimicry of other aggregation-prone peptides that drive pathogenic protein assembly.

INTRODUCTION

The higher-order assembly of proteins rich in β structure is correlated with poor prognosis in several neurodegenerative diseases.¹⁻⁴ Intracellular accumulation of the tau protein into neurofibrillary tangles (NFTs) is linked to cognitive dysfunction in over 20 disorders collectively termed 'tauopathies'.⁵⁻⁹ The normal function of tau is to stabilize microtubules (MTs), the support structures in axons.^{10,11} Pathogenic misfolding and aggregation can be caused by mutations in the *MAPT* gene that encodes for tau or by aberrant post-translational modifications.¹²⁻¹⁶ While toxicity has been associated with various forms of aggregated tau, current data supports oligomeric species as a primary driver of neuronal death.¹⁷ It is now accepted that tau pathology becomes self-perpetuating, with the capacity to spread from neuron to neuron and cause normal tau to become misfolded (Figure 1A).¹⁸⁻²⁴ Controlling the processes that govern tau fibrilization and cellular propagation is critical for understanding the progression of tauopathies.

Tau is an intrinsically disordered protein harboring up to four MT-binding repeat domains (R1-R4) in the C-terminal half. Like many amyloidogenic proteins, tau fibrilization involves conformational reorganization into β -rich folds, followed by supramolecular assembly into layered parallel β -sheets (Figure 1B).^{25-28,4} This assembly is driven by favorable H-bonding and hydrophobic interactions between well-defined aggregation-prone hexapeptide motifs in the R2 (275VQIINK₂₈₀; PHF6*) and R3 (306VQIVYK₃₁₁; PHF6) domains, which are also essential for MT binding. Short peptide models have long been used to

study the structure and function of tau aggregates *in vitro*. Direct inhibitors of tau fibrilization are largely limited to dyes and other redox-active aromatic compounds.²⁹ The aggregation-prone R2/R3 segments have more recently been used in the structure-based design of modified peptides that inhibit the aggregation of a PHF6 hexapeptide or truncated forms of recombinant tau.³⁰⁻³⁴ One group recently described a series of peptides capable of blocking the aggregation of full-length tau and as well as seeding in cells.^{35,36} Conformationally rigid and proteolytically stable peptidomimetics may hold particular promise as

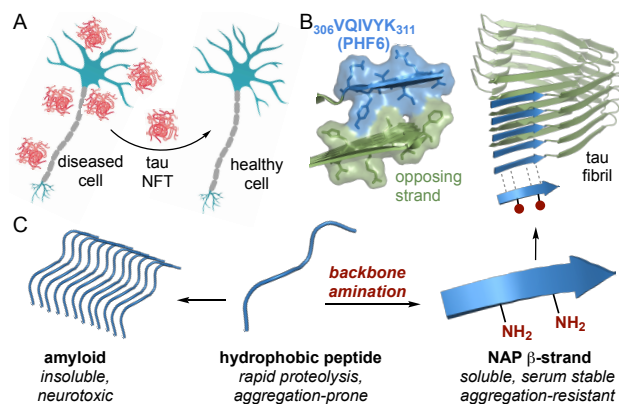


Figure 1. (A) Propagation of tau NFTs from neuron to neuron. (B) Cross- β sidechain interactions of PHF6 and parallel β -sheet stacking in a tau fibril. (C) N-Amino peptide (NAP) mimics of aggregation-prone peptides.

ligands of tau and other amyloid proteins that are difficult to target in a sequence-specific manner.

Despite examples of peptidomimetic disruptors of β -sheet-mediated protein interactions, strategies to translate conformationally extended peptide leads into inhibitors remain limited.^{37,38} This is due in part to the flexibility of short peptide sequences, coupled with the large surface areas and diverse modes of β -sheet interactions.³⁹ The propensity for conformationally extended peptides to aggregate via exposed H-bonding edges presents another significant challenge in the design of soluble β -strand mimics.⁴⁰ Presentation of a β -strand epitope for protein recognition typically relies on the templating effect of an auxiliary β -strand (as in linear and macrocyclic β -hairpins), intra-strand conformational restriction through covalent tethering, or backbone amide N-alkylation to preclude strand self-aggregation. While backbone amide substitution allows for retention of side chain information, N-methylation (or incorporation of Pro) can promote main chain torsions incompatible with β -sheet mimicry. We recently described an approach to β -strand stabilization based on peptide backbone N-amination (Figure 1C).⁴¹ The conformational and non-aggregating characteristics of N-amino peptides (NAPs) are consistent across distinct models of β -sheet folding and are attributed to cooperative non-covalent interactions involving the $N\alpha$ -NH₂ substituent. Here, we describe the design and synthesis of NAPs that block tau fibrilization and spread in a sequence-specific manner. Our N-amination strategy enables the use of tau filament structure to guide the design of its own peptidomimetic ligands. Using biophysical and cellular propagation assays, we demonstrate the utility of a minimalist β -strand mimicry approach to target β -rich amyloids.

RESULTS

Design and Synthesis of NAP-based Tau Ligands. The R3₃₀₆VQIVYK₃₁₁ hexapeptide motif is widely accepted as the key amyloidogenic core of tau because filaments formed from this motif closely resemble those observed from Alzheimer's disease tau.^{27,42,43} However, recent crystal structures of the R2₂₇₅VQIINK₂₈₀ motif show tighter side chain packing and strand interdigitation relative to the R3 hexapeptide, suggesting it to be a more powerful driver of tau aggregation.³⁵ Since the specific contribution of individual residues in these sequences have not yet been studied, we chose to perform a complete backbone N-amino scan along the length of each hexapeptide. Our NAP-based library included mono-, di-, and tri-N-aminated analogues. We limited poly-N-amino peptides to those harboring amide substitutions on a single H-bonding edge, thus retaining a fully intact edge for interaction with tau.

We synthesized 14 NAP β -strand mimics on solid support as described in Figure 2. We excluded analogues harboring N-amino glutamine (aGln) or N-amino aspartagine (aAsn) residues since these undergo rapid intrasidic cyclization via the hydrazide during cleavage.⁴⁴ Our strategy relied on incorporation of orthogonally-protected N-amino dipeptide building blocks that are available in 3 steps from the corresponding α -amino benzyl esters. Notably, this dipeptide fragment approach allows for Fmoc SPPS of NAPs using automated, microwave-assisted HCTU/NMM condensation protocols on Rink amide MBHA resin. In contrast to canonical dipeptide (or larger) fragments, N-aminated building blocks are highly resistant to racemization during activation owing to the electron-withdrawing NHBoc

substituent.⁴⁵ Following elongation, NAPs were cleaved from the resin and purified by preparative RP-HPLC. All NAPs were characterized by ¹H NMR and HRMS. The parent unmodified hexapeptides **AcPHF6** and **AcPHF6*** were also synthesized for comparison to backbone-aminated variants.

NAP Tau Mimics Inhibit Tau Fibrilization *in Vitro*. We chose thioflavin T (ThT), an amyloid specific fluorescent dye that binds to β -sheet assemblies, to first evaluate the effect of NAPs on recombinant tau aggregation. For these studies we expressed and purified full-length tau featuring a P301L mutation (Figure S1) frequently observed in patients with frontotemporal dementia and parkinsonism linked to chromosome 17 (FTDP-17).⁴⁶ This missense mutation leads to local structure destabilization around the amyloid forming region resulting in faster aggregation. Recombinant tau_{P301L} aggregated in the presence of equimolar heparin sulfate ($t_{1/2} = 6.5 \pm 0.4$ h) starting with a very short 0.5 h lag phase followed by a 24 h exponential growth phase. Of the 14 NAPs tested, 6 were found to significantly reduce end-point ThT fluorescence of tau_{P301L} when incubated at 2-fold molar excess (Figures 3A and S2A). Compounds **2** and **4** are mono- and di-aminated hexapeptides derived from the R2 PHF6* aggregation-prone sequence, whereas compounds **5**, **6**, **12**, and **13** are each derived from the R3 PHF6 sequence. Several other NAPs had no effect on end-point ThT fluorescence or lacked consistent inhibition across repeated experiments (Figure S2B-C). In agreement with previous reports,^{47,35} we observed significant aggregation of both the R2 and R3 parent peptides (**AcPHF6*** and **AcPHF6**) when incubated alone in aq. NaOAc buffer, as evidenced by intense ThT fluorescence after 48 h (Figure 3B). In contrast, the 6 NAP inhibitors mentioned

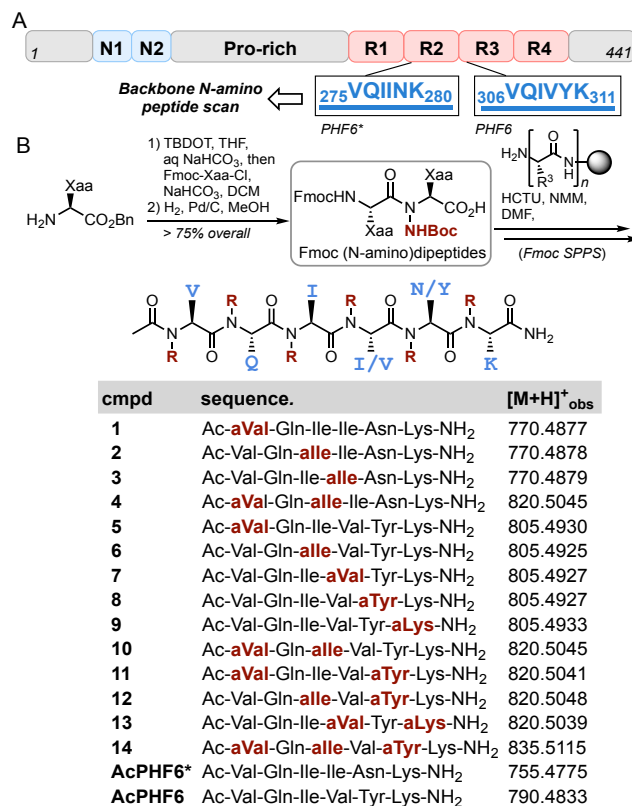


Figure 2. N-Amino peptide scan of tau hexapeptides. (A) Aggregation-prone tau parent sequences; (B) NAP analogues of PHF6 and PHF6* prepared by SPPS.

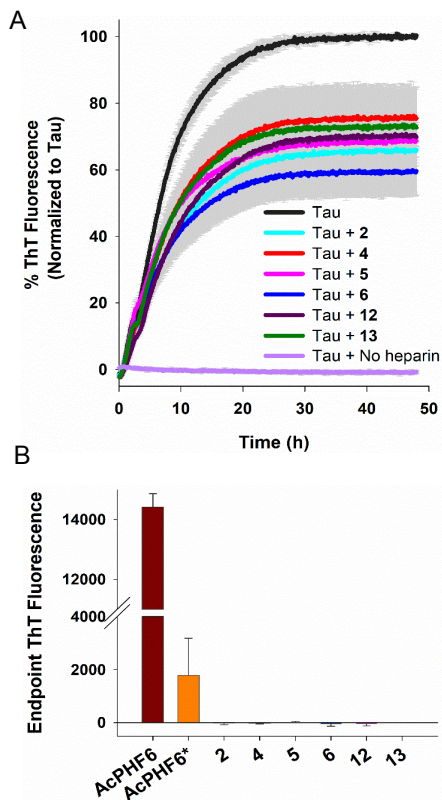


Figure 3. Inhibition of tau_{P301L} aggregation and monomeric nature of inhibitors examined using thioflavin T fluorescence: (A) Incubation of 20 μ M inhibitors with 10 μ M heparin-treated tau_{P301L} significantly reduced ThT fluorescence. (B) N-amino substitution completely abolished the aggregation propensity of AcPHF6 and AcPHF6* as determined by negligible ThT fluorescence after 48 h.

above (**2**, **4-6**, **12**, and **13**) exhibited no such fluorescence, suggesting that even a single backbone N-amino group was sufficient to confer resistance to self-aggregation.

To confirm the effect of NAPs on tau fibril growth, we used transmission electron microscopy (TEM) to visualize the morphology and maturity of fibrillar species. Heparin-induced tau_{P301L} fibrils were allowed to grow over 96 h in the presence or absence of inhibitors. Untreated tau_{P301L} afforded large, helical, amyloid-like filamentous fibrils. In contrast, we did not observe any elongated or mature fibrils in the presence of a two-fold molar excess of the 6 NAP inhibitors mentioned above. Di-N-aminated peptides **4**, **12**, and **13** were particularly effective at

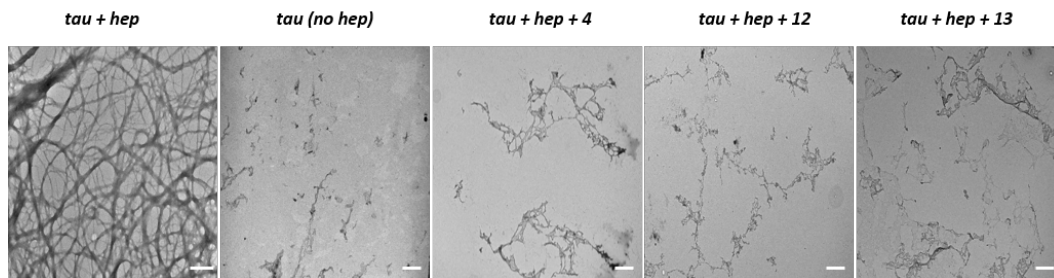


Figure 4. Fibril morphology under transmission electron microscope. Left to right: Incubation of 10 μ M tau_{P301L} resulted in large, mature and filamentous fibrils only in the presence of heparin. Addition of 20 μ M of NAP inhibitors **4**, **12**, and **13** afforded non-fibrillary amorphous aggregates similar to control. Scale bar represent a distance 500 nm in the tau+hep panel and 2 μ m in the other panels.

blocking fibrilization, resulting in non-fibrillary amorphous aggregates similar to control wells containing tau_{P301L} without heparin (Figure 4). In the case of the mono-N-aminated peptides (**2**, **5**, and **6**) we observed short, immature rod-like fibrils, indicative of a more modest effect on tau assembly (Figure S3).

Di-N-aminated Hexapeptides Block the Cellular Transmission of Tau Fibrils. Recent studies show that extracellular tau fibrils spread in a prion-like fashion from one cell to the next.¹⁸⁻²⁴ This mode of propagation is important for the spread of NFTs, neuropil threads, and plaque-associated neurites – all of which contribute to the progression of Alzheimer’s disease. To test whether NAP inhibitors are able to block the seeding activity of recombinant tau_{P301L}, we employed HEK293 biosensor cells that stably express a tau-yellow fluorescent protein fusion (tau-RD(LM)-YFP).^{21,22} When we treated these cells with preformed heparin-induced fibrils of tau_{P301L} we observed a large number of intracellular tau aggregates as indicated by punctate fluorescence after 48 h. These wells exhibited a mean of 38% aggregate-containing cells over 3 separate experiments, demonstrating the ability for fibrillar tau_{P301L} to enter cells and seed the aggregation of the endogenous tau-RD(LM)-YFP (Figure 5 and S4). Given their superior anti-fibrillar activity by TEM and reduced peptide character, we elected to carry out cell seeding experiments with di-N-aminated peptides **4**, **12**, and **13**. Pre-treatment of monomeric tau_{P301L} with 1.9 μ M of di-NAPs **12** and **13** (derived from the R3 PHF6 motif) significantly reduced seeding capacity. This effect was less pronounced at 0.009 μ M. Inhibitor **4**, derived from the R2 domain PHF6* motif exhibited far weaker anti-seeding activity at both high and low concentrations (Figures 5 and S4).

Given that pathogenic tau can be secreted from cells in various forms (as oligomers, aggregates, or mature fibrils⁴⁸), we tested whether NAPs could cap pre-formed tau fibrils to block cellular transmission. In this experiment NAPs were incubated with mature tau_{P301L} fibrils for 36 h prior to treatment of cells expressing tau-RD(LM)-YFP. Indeed, we found that compounds **12** and **13** were able to effectively inhibit propagation in a dose-dependent manner. We determined a fibril capping IC₅₀ in cells in the 5 μ M range across 3 repeated experiments (Figures 6 and S5). These results demonstrate that our structure-based NAP mimicry approach afford ligands with anti-seeding activity irrespective of tau aggregation state.

Consistent with the seeding experiments above using monomeric tau_{P301L}, di-NAP **4** was generally ineffective at capping pre-formed fibrils and blocking propagation (Figures 6 and S5). We then considered the possibility that di-NAPs **12** and **13** may

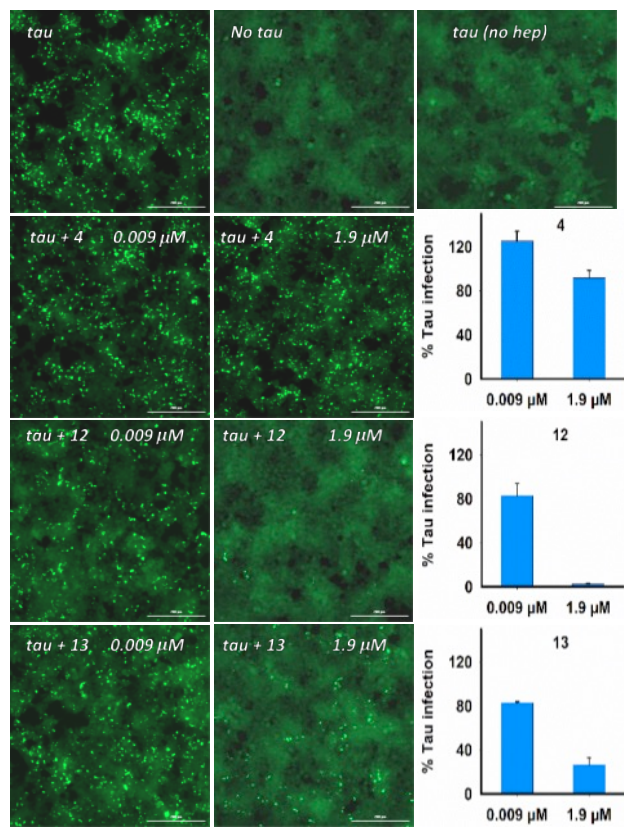


Figure 5. Inhibition of $\text{tau}_{\text{P301L}}$ aggregation and seeding. Soluble monomeric $\text{tau}_{\text{P301L}}$ (0.19 μM) in the presence of heparin was co-incubated with 0.009 μM or 1.9 μM of inhibitors for 4 days, then added to HEK293 cells stably expressing tau-RD (P301L/V337M)-YFP. Fibrillized $\text{tau}_{\text{P301L}}$ can induce aggregation of endogenous tau in cells seen as focal puncta with high fluorescence. Shown here are representative images of cells, at $20\times$ magnification under FITC channel. Treatment with 1.9 μM of either **12** or **13** was sufficient to prevent seeding, however **4** was found to be ineffective. Scale bar represents 200 μm . Bar graphs show the number of intracellular fluorescent punctates relative to control infection wells lacking inhibitor.

be entering cells and inhibiting seeding by interacting with endogenous tau-RD(LM)-YFP, rather than capping extracellular pre-formed fibrils. We thus repeated the experiment without the 36 h inhibitor + mature fibril co-incubation period. Both di-NAPs **12** and **13** failed to inhibit endogenous tau aggregation in this experiment, suggesting that the compounds interact with extracellular $\text{tau}_{\text{P301L}}$ to block cellular transmission (Figure S6).

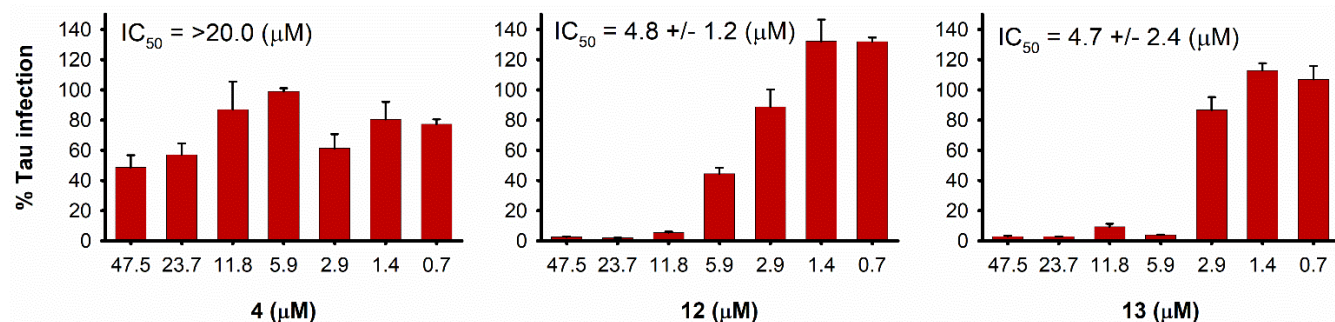


Figure 6. Concentrations of NAP inhibitors required to cap pre-formed 0.19 μM $\text{tau}_{\text{P301L}}$ fibrils and block seeding in HEK293 cells expressing tau-RD (P301L/V337M)-YFP. Mature fibrils were treated with various concentrations of NAPs for 36 h, added to cells, and incubated for an additional 48 h. Punctate fluorescence was quantified to derive % tau infection relative to fibrils untreated with NAPs.

Di-NAPs are Stable in Human Serum and Non-Toxic to Neuronal Cells. Compounds **12** and **13** feature two hydrazide bonds within the peptidomimetic backbone. Their utility as tau ligands in cell-based experiments would benefit from resistance to proteolytic degradation. We carried out stability studies in human serum and monitored degradation by RP-HPLC (Figure 7A). Both **12** and **13** were found to be remarkably stable in 25% human serum (> 83% intact after 24 h). In contrast, an eight-residue control peptide was rapidly degraded over 24 h in the same assay. Although the parent **AcPHF6** peptide could not be used as a control due to rapid self-aggregation, the stability of **12** and **13** demonstrates the ability of N-amination to protect against peptide backbone degradation.

Cellular seeding experiments with $\text{tau}_{\text{P301L}}$ in the presence or absence of di-NAPs **12** and **13** did not result in detectable toxicity to HEK293 biosensor cells (Figure S7A). We carried out MTT assay to ensure that inhibitors **12** and **13** are not toxic to human neural cells. As shown in Figure 7B, **12** and **13** exhibited no appreciable toxicity toward SH-SY5Y (human neuroblastoma) cells up to 50 μM , or 10-fold their anti-seeding IC_{50} values.

N-Amination Imparts Backbone Conformational Constraint in Solution. Di-NAPs that cap mature tau fibrils are expected to adopt parallel β -sheet-like conformations. X-ray crystallography of a model di-N-aminated tripeptide previously demonstrated its self-association as a dimeric species with extended backbone geometries.⁴¹ To gain insight into the solution structure of our lead tau ligands, we carried out 2D-NMR spectroscopy followed by simulated annealing. While **AcPHF6** was insoluble in water, we were able to obtain gCOSY, TOCSY, and ROESY NMR spectra in 9:1 $\text{H}_2\text{O}:\text{D}_2\text{O}$ for **12** and **13**. ^1H NMR spectra were remarkably well resolved and devoid of significant minor rotamers despite the presence of two N-substituted amide bonds. Moreover, inter-residue NOEs were limited to correlations consistent with an extended solution conformation ($\text{C}\alpha\text{H}_i \rightarrow \text{NH}_{i+1}$). Though short linear peptides are expected to be highly flexible in solution, the absence of characteristic turn correlations suggests conformational restriction imparted by the N-amino groups. Distance-restrained simulated annealing and clustering based on backbone dihedral angles afforded ensembles of the three most populated conformers of **12** (Figure 8). These clusters revealed high convergence of ϕ and ψ torsions within the Gln2 and Val4 residues to the β -sheet region of Ramachandran space. In contrast, the N-aminated allele3

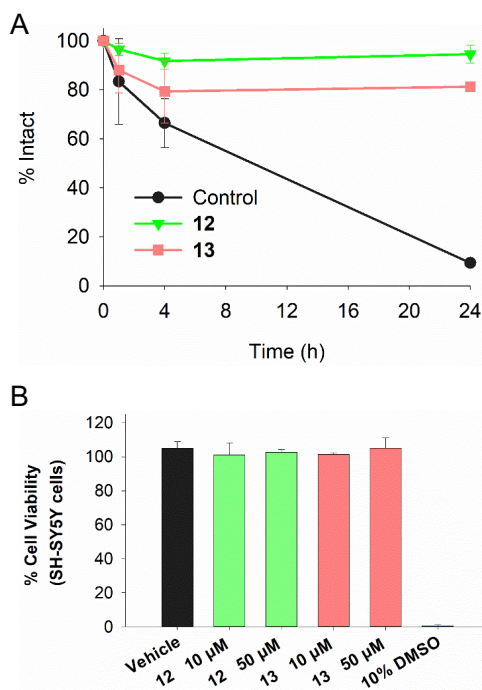


Figure 7. Serum stability and cytotoxicity of NAP inhibitors. (A) NAPs **12** and **13** remained >80% intact after 24 h incubation in 25% human serum, whereas control peptide (H-LITRLENT-NH₂) was rapidly degraded, as measured by HPLC. (B) NAPs **12** and **13** did not exhibit any appreciable toxicity toward human neuroblastoma (SH-SY5Y) cells at low (10 μ M) or high (50 μ M) concentration after 48 h, as determined by MTT assay.

and aTyr5 residues exhibit greater conformational heterogeneity. This pattern was also observed in the case of di-NAP **13** (Figure S8). To specifically parse the conformational impact of N-amination, we carried out unrestrained conventional MD

simulations on **12** and AcPHF6. Ramachandran plots for the 400 ns simulation again showed that N-amination severely restricts accessible backbone torsions of the preceding residue (Figure S9). We previously showed that NAPs readily engage in intrasidue C6 H-bonds between the N-NH₂ donor and the carbonyl O acceptor, even in protic solvent.⁴⁹ Coupled with the constraint imposed on the preceding residue, the hydrazide bond thus may serve to further stabilize β -sheet-like conformations that recognize fibrillar tau.

Di-NAP **12** Does Not Inhibit A β ₄₂ Aggregation *in Vitro*.

Many small molecule protein aggregation inhibitors exhibit undesired promiscuity. A peptidomimetic approach to tau inhibition offers prospects for achieving selectivity over other amyloids rich in β structure. As a preliminary test, we selected our best-performing aggregation-inhibitory tau mimic, **12**, and determined its effect on A β ₄₂ aggregation *in vitro* (Figure 9). Incubation of synthetic, full-length A β ₄₂ (40 μ M) in the presence of ThT and various concentrations of **12** resulted in strong fluorescence indicative of aggregation. Di-NAP **12** exhibited no inhibitory effect on A β ₄₂ aggregation up to a 4-fold molar excess (160 μ M). We similarly observed no effect on lag-time at any of the concentrations tested. Compound **12** thus exhibits *in vitro* selectivity for tau over A β ₄₂, an amyloid whose parallel β -sheet assembly also driven by a hydrophobic hexapeptide core motif.

CONCLUSION

We have described the design, synthesis, and biological evaluation of a novel class of β -strand mimics that block tau aggregation and propagation. Using an amide-to-hydrazide replacement strategy, we carried out a positional scan of aggregation-prone peptide sequences derived from the R2 and R3 domain of tau. Several NAP analogues inhibited the fibrilization of recombinant full-length tau as well as its seeding capacity in an in-cell

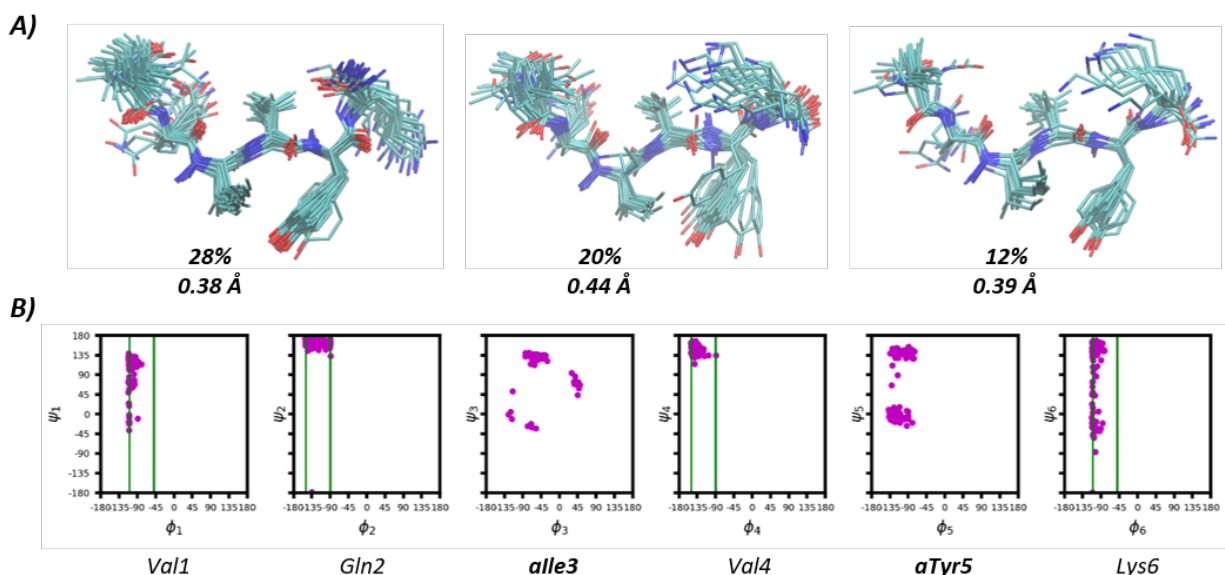


Figure 8. Solution NMR-derived structural ensemble of **12**. (A) Sequential and medium to long-range NOEs observed in the ROESY spectrum along with $^3J_{\text{NH-C}\alpha\text{H}}$ coupling constant were used to derive distance and dihedral restraints for simulated annealing. About one hundred energy-minimized structures were calculated and grouped into eighteen clusters. Structures of top three clusters are shown with their populations and average backbone RMSD relative to the cluster average. (B) Residue-wise Ramachandran plots for the solution-derived structural ensemble. Green lines mark the dihedral restraints derived from the $^3J_{\text{NH-C}\alpha\text{H}}$ coupling constants.

aggregation assay. Key features of the described NAP inhibitors

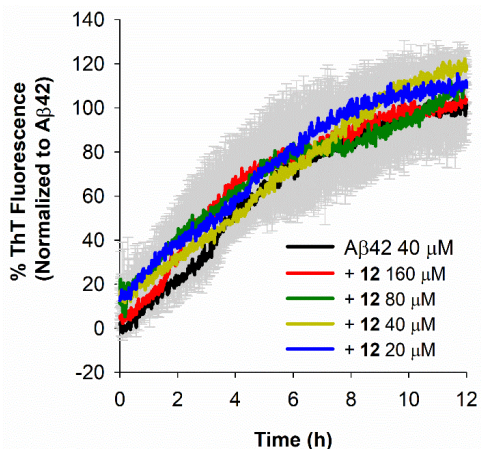


Figure 9. ThT fluorescence assay with $A\beta_{42}$ in the presence or absence of **12** showed no inhibitory effect on $A\beta_{42}$ aggregation.

include increased conformational rigidity, resistance toward self-aggregation, and remarkable stability toward serum proteases. Our most effective inhibitor of tau fibrilization and seeding showed no effect on the *in vitro* aggregation of $A\beta_{42}$. Discrimination between structurally related β -rich assemblies is potentially enabled by NAPs, which exhibit a full complement of side chains in a minimalist single-strand design. In using the sequence of tau to guide the design of its own inhibitors, our work sets the stage for the development of selective ligands of other pathogenic amyloids. Given that disease-associated conformational strains of tau are known to propagate *in vivo* with high fidelity, we also expect that a NAP-based strategy can be used to target unique structural motifs within such polymorphs.^{50,51} The current study thus provides a rational basis for the design of soluble β -strand mimics with high levels of specificity.

ASSOCIATED CONTENT

Supporting Information

The Supporting Information is available free of charge on the ACS Publications website.

Supplementary figures, Experimental procedures, and compound characterizations (PDF)

AUTHOR INFORMATION

Corresponding Author

* Email: jdelvalle@nd.edu

Author Contributions

The manuscript was written through contributions of all authors and all authors have given approval to the final version of the manuscript.

Funding Sources

National Science Foundation (CHE 2021265) and National Institutes of Health (R01GM124160)

ACKNOWLEDGMENT

We thank Dr. Marc Diamond (UT Southwestern) for generously providing tau-RD(LM)-YFP biosensor cells and Dr. Laura Blair (University of South Florida) for providing tau_{P301L} expression plasmid and SH-SY5Y cells. This work was supported by a grant from the National Science Foundation (NSF CHE2021265 to J. R. D.) and the National Institute of General Medical Sciences (NIH R01GM124160 to Y.S.L.)

REFERENCES

- [1] Goate, A.; Chartier-Harlin, M. C.; Mullan, M.; Brown, J.; Crawford, F.; Fidani, L.; Giuffra, L.; Haynes, A.; Irving, N.; James, L.; et al. Segregation of a missense mutation in the amyloid precursor protein gene with familial Alzheimer's disease. *Nature* **1991**, *349*, 704-706.
- [2] Braak, H.; Alafuzoff, I.; Arzberger, T.; Kretschmar, H.; Del Tredici, K. Staging of Alzheimer disease-associated neurofibrillary pathology using paraffin sections and immunocytochemistry. *Acta Neuropathol.* **2006**, *112*, 389-404.
- [3] Knowles, T. P. J.; Vendruscolo, M.; Dobson, C. M. The amyloid state and its association with protein misfolding diseases. *Nature Rev. Mol. Cell Biol.* **2014**, *15*, 384-396.
- [4] Iadanza, M. G.; Jackson, M. P.; Hewitt, E. W.; Ranson, N. A.; Radford, S. E. A new era for understanding amyloid structures and disease. *Nature Rev. Mol. Cell Biol.* **2018**, *19*, 755-773.
- [5] Wood, J. G.; Mirra, S. S.; Pollock, N. J.; Binder, L. I. Neurofibrillary tangles of Alzheimer disease share antigenic determinants with the axonal microtubule-associated protein tau (tau). *Proc. Natl. Acad. Sci. USA* **1986**, *83*, 4040-4043.
- [6] Goedert, M.; Spillantini, M. G.; Jakes, R.; Rutherford, D.; Crowther, R. A. Multiple isoforms of human microtubule-associated protein tau: sequences and localization in neurofibrillary tangles of Alzheimer's disease. *Neuron* **1989**, *3*, 519-526.
- [7] Crowther, R. A.; Olesen, O. F.; Jakes, R.; Goedert, M. The microtubule binding repeats of tau protein assemble into filaments like those found in Alzheimer's disease. *FEBS Lett.* **1992**, *309*, 199-202.
- [8] Virginia M-Y Lee; Michel Goedert; Trojanowski, J. Q. Neurodegenerative Tauopathies. *Ann. Rev. Neurosci.* **2001**, *24*, 1121-1159.
- [9] Goedert, M.; Eisenberg, D. S.; Crowther, R. A. Propagation of Tau Aggregates and Neurodegeneration. *Annu. Rev. Neurosci.* **2017**, *40*, 189-210.
- [10] Weingarten, M. D.; Lockwood, A. H.; Hwo, S. Y.; Kirschner, M. W. A protein factor essential for microtubule assembly. *Proc. Natl. Acad. Sci. USA* **1975**, *72*, 1858-1862.
- [11] Lee, G.; Neve, R. L.; Kosik, K. S. The microtubule binding domain of tau protein. *Neuron* **1989**, *2*, 1615-1624.
- [12] Grundke-Iqbal, I.; Iqbal, K.; Tung, Y. C.; Quinlan, M.; Wisniewski, H. M.; Binder, L. I. Abnormal phosphorylation of the microtubule-associated protein tau (tau) in Alzheimer cytoskeletal pathology. *Proc. Natl. Acad. Sci. USA* **1986**, *83*, 4913-4917.
- [13] Neve, R. L.; Harris, P.; Kosik, K. S.; Kurmit, D. M.; Donlon, T. A. Identification of cDNA clones for the human microtubule-associated protein tau and chromosomal localization of the genes for tau and microtubule-associated protein 2. *Brain Res.* **1986**, *387*, 271-280.
- [14] Goedert, M.; Spillantini, M. G.; Cairns, N. J.; Crowther, R. A. Tau proteins of Alzheimer paired helical filaments: abnormal phosphorylation of all six brain isoforms. *Neuron* **1992**, *8*, 159-168.
- [15] Morris, M.; Knudsen, G. M.; Maeda, S.; Trinidad, J. C.; Ioanoviciu, A.; Burlingame, A. L.; Mucke, L. Tau post-translational modifications in wild-type and human amyloid precursor protein transgenic mice. *Nat. Neurosci.* **2015**, *18*, 1183-1189.
- [16] Arakhamia, T.; Lee, C. E.; Carlomagno, Y.; Duong, D. M.; Kundinger, S. R.; Wang, K.; Williams, D.; DeTure, M.; Dickson, D. W.; Cook, C. N.; Seyfried, N. T.; Petrucelli, L.; Fitzpatrick, A. W. P. Posttranslational Modifications Mediate the Structural Diversity of Tauopathy Strains. *Cell* **2020**, *180*, 633-644.e612.

- [17] Maeda, S.; Sahara, N.; Saito, Y.; Murayama, S.; Ikai, A.; Takashima, A. Increased levels of granular tau oligomers: an early sign of brain aging and Alzheimer's disease. *Neurosci. Res.* **2006**, *54*, 197-201.
- [18] Frost, B.; Jacks, R. L.; Diamond, M. I. Propagation of tau misfolding from the outside to the inside of a cell. *J. Bio. Chem.* **2009**, *284*, 12845-12852.
- [19] Kfoury, N.; Holmes, B. B.; Jiang, H.; Holtzman, D. M.; Diamond, M. I. Trans-cellular propagation of Tau aggregation by fibrillar species. *J. Bio. Chem.* **2012**, *287*, 19440-19451.
- [20] Spillantini, M. G.; Goedert, M. Tau pathology and neurodegeneration. *Lancet Neurol.* **2013**, *12*, 609-622.
- [21] Sanders, D. W.; Kaufman, S. K.; DeVos, S. L.; Sharma, A. M.; Mirbaha, H.; Li, A.; Barker, S. J.; Foley, A. C.; Thorpe, J. R.; Serpell, L. C.; Miller, T. M.; Grinberg, L. T.; Seeley, W. W.; Diamond, M. I. Distinct tau prion strains propagate in cells and mice and define different tauopathies. *Neuron* **2014**, *82*, 1271-1288.
- [22] Holmes, B. B.; Furman, J. L.; Mahan, T. E.; Yamasaki, T. R.; Mirbaha, H.; Eades, W. C.; Belaygorod, L.; Cairns, N. J.; Holtzman, D. M.; Diamond, M. I. Proteopathic tau seeding predicts tauopathy in vivo. *Proc. Natl. Acad. Sci. USA* **2014**, *111*, E4376.
- [23] Mirbaha, H.; Chen, D.; Morazova, O. A.; Ruff, K. M.; Sharma, A. M.; Liu, X.; Goodarzi, M.; Pappu, R. V.; Colby, D. W.; Mirzaei, H.; Joachimiak, L. A.; Diamond, M. I. Inert and seed-competent tau monomers suggest structural origins of aggregation. *eLife* **2018**, *7*, e36584.
- [24] Gibbons, G. S.; Lee, V. M. Y.; Trojanowski, J. Q. Mechanisms of Cell-to-Cell Transmission of Pathological Tau A Review. *JAMA Neurol.* **2019**, *76*, 101-108.
- [25] Wischik, C. M.; Novak, M.; Edwards, P. C.; Klug, A.; Tichelaar, W.; Crowther, R. A. Structural characterization of the core of the paired helical filament of Alzheimer disease. *Proc. Natl. Acad. Sci. USA* **1988**, *85*, 4884-4888.
- [26] Wischik, C. M.; Novak, M.; Thøgersen, H. C.; Edwards, P. C.; Runswick, M. J.; Jakes, R.; Walker, J. E.; Milstein, C.; Roth, M.; Klug, A. Isolation of a fragment of tau derived from the core of the paired helical filament of Alzheimer disease. *Proc. Natl. Acad. Sci. USA* **1988**, *85*, 4506-4510.
- [27] von Bergen, M.; Friedhoff, P.; Biernat, J.; Heberle, J.; Mandelkow, E. M.; Mandelkow, E. Assembly of tau protein into Alzheimer paired helical filaments depends on a local sequence motif ((306)VQIVYK(311)) forming beta structure. *Proc. Natl. Acad. Sci. USA* **2000**, *97*, 5129-5134.
- [28] Berriman, J.; Serpell, L. C.; Oberg, K. A.; Fink, A. L.; Goedert, M.; Crowther, R. A. Tau filaments from human brain and from in vitro assembly of recombinant protein show cross-beta structure. *Proc. Natl. Acad. Sci. USA* **2003**, *100*, 9034-9038.
- [29] Brunden, K. R.; Trojanowski, J. Q.; Lee, V. M. Y. Advances in tau-focused drug discovery for Alzheimer's disease and related tauopathies. *Nat. Rev. Drug Disc.* **2009**, *8*, 783-793.
- [30] Zheng, J.; Liu, C.; Sawaya, M. R.; Vadla, B.; Khan, S.; Woods, R. J.; Eisenberg, D.; Goux, W. J.; Nowick, J. S. Macrocyclic β -Sheet Peptides That Inhibit the Aggregation of a Tau-Protein-Derived Hexapeptide. *J. Am. Chem. Soc.* **2011**, *133*, 3144-3157.
- [31] Sievers, S. A.; Karanicolas, J.; Chang, H. W.; Zhao, A.; Jiang, L.; Zirafi, O.; Stevens, J. T.; Münch, J.; Baker, D.; Eisenberg, D. Structure-based design of non-natural amino-acid inhibitors of amyloid fibril formation. *Nature* **2011**, *475*, 96-100.
- [32] Dammers, C.; Yolcu, D.; Kukuk, L.; Willbold, D.; Pickhardt, M.; Mandelkow, E.; Horn, A. H. C.; Sticht, H.; Malhis, M. N.; Will, N.; Schuster, J.; Funke, S. A. Selection and Characterization of Tau Binding D-Enantiomeric Peptides with Potential for Therapy of Alzheimer Disease. *PLoS ONE* **2016**, *11*, e0167432.
- [33] Wang, C. K.; Northfield, S. E.; Huang, Y. H.; Ramos, M. C.; Craik, D. J. Inhibition of tau aggregation using a naturally-occurring cyclic peptide scaffold. *Eur. J. Med. Chem.* **2016**, *109*, 342-349.
- [34] Chemerovski-Glikman, M.; Frenkel-Pinter, M.; Mdah, R.; Abu-Mokh, A.; Gazit, E.; Segal, D. Inhibition of the Aggregation and Toxicity of the Minimal Amyloidogenic Fragment of Tau by Its Pro-Substituted Analogues. *Chem. Eur. J.* **2017**, *23*, 9618-9624.
- [35] Seidler, P. M.; Boyer, D. R.; Rodriguez, J. A.; Sawaya, M. R.; Cascio, D.; Murray, K.; Gonen, T.; Eisenberg, D. S. Structure-based inhibitors of tau aggregation. *Nat. Chem.* **2018**, *10*, 170-176.
- [36] Seidler, P. M.; Boyer, D. R.; Murray, K. A.; Yang, T. P.; Bentzel, M.; Sawaya, M. R.; Rosenberg, G.; Cascio, D.; Williams, C. K.; Newell, K. L.; Ghetti, B.; DeTure, M. A.; Dickson, D. W.; Vinters, H. V.; Eisenberg, D. S. Structure-based inhibitors halt prion-like seeding by Alzheimer's disease-and tauopathy-derived brain tissue samples. *J. Biol. Chem.* **2019**, *294*, 16451-16464.
- [37] Loughlin, W. A.; Tyndall, J. D. A.; Glenn, M. P.; Hill, T. A.; Fairlie, D. P. Update 1 of: Beta-Strand Mimetics. *Chem. Rev.* **2010**, *110*, PR32-PR69.
- [38] Laxio Arenas, J.; Kaffy, J.; Ongeri, S. Peptides and peptidomimetics as inhibitors of protein-protein interactions involving β -sheet secondary structures. *Curr. Opin. Chem. Biol.* **2019**, *52*, 157-167.
- [39] Watkins, A. M.; Arora, P. S. Anatomy of beta-strands at protein-protein interfaces. *ACS Chem. Biol.* **2014**, *9*, 1747-1754.
- [40] Chiti, F.; Stefani, M.; Taddei, N.; Ramponi, G.; Dobson, C. M. Rationalization of the effects of mutations on peptide and protein aggregation rates. *Nature* **2003**, *424*, 805-808.
- [41] Sarnowski, M. P.; Kang, C. W.; Elbatrawi, Y. M.; Wojtas, L.; Del Valle, J. R. Peptide N-Amination Supports β -Sheet Conformations. *Angew. Chem. Int. Ed.* **2017**, *56*, 2083-2086.
- [42] von Bergen, M.; Barghorn, S.; Li, L.; Marx, A.; Biernat, J.; Mandelkow, E. M.; Mandelkow, E. Mutations of tau protein in frontotemporal dementia promote aggregation of paired helical filaments by enhancing local beta-structure. *J. Biol. Chem.* **2001**, *276*, 48165-48174.
- [43] Fitzpatrick, A. W. P.; Falcon, B.; He, S.; Murzin, A. G.; Murshudov, G.; Garringer, H. J.; Crowther, R. A.; Ghetti, B.; Goedert, M.; Scheres, S. H. W. Cryo-EM structures of tau filaments from Alzheimer's disease. *Nature* **2017**, *547*, 185-190.
- [44] Kang, C. W.; Ranatunga, S.; Sarnowski, M. P.; Del Valle, J. R. Solid-phase synthesis of tetrahydropyridazinedione-constrained peptides. *Org. Lett.* **2014**, *16*, 5434-5437.
- [45] Rathman, B. M.; Allen, J. L.; Shaw, L. N.; Del Valle, J. R. Synthesis and biological evaluation of backbone-aminated analogues of gramicidin S. *Bioorg. Med. Chem. Lett.* **2020**, *30*, 127283.
- [46] Hutton, M.; Lendon, C. L.; Rizzu, P.; Baker, M.; Froelich, S.; Houlden, H.; Pickering-Brown, S.; Chakraverty, S.; Isaacs, A.; Grover, A.; Hackett, J.; Adamson, J.; Lincoln, S.; Dickson, D.; Davies, P.; Petersen, R. C.; Stevens, M.; de Graaff, E.; Wauters, E.; van Baren, J.; Hillebrand, M.; Joosse, M.; Kwon, J. M.; Nowotny, P.; Che, L. K.; Norton, J.; Morris, J. C.; Reed, L. A.; Trojanowski, J.; Basun, H.; Lannfelt, L.; Neystat, M.; Fahn, S.; Dark, F.; Tannenberg, T.; Dodd, P. R.; Hayward, N.; Kwok, J. B. J.; Schofield, P. R.; Andreadis, A.; Snowden, J.; Craufurd, D.; Neary, D.; Owen, F.; Oostra, B. A.; Hardy, J.; Goate, A.; van Swieten, J.; Mann, D.; Lynch, T.; Heutink, P. Association of missense and 5'-splice-site mutations in tau with the inherited dementia FTDP-17. *Nature* **1998**, *393*, 702-705.
- [47] Sawaya, M. R.; Sambashivan, S.; Nelson, R.; Ivanova, M. I.; Sievers, S. A.; Apostol, M. I.; Thompson, M. J.; Balbirnie, M.; Wiltzius, J. J. W.; McFarlane, H. T.; Madsen, A. Ø.; Riekel, C.; Eisenberg, D. Atomic structures of amyloid cross- β spines reveal varied steric zippers. *Nature* **2007**, *447*, 453-457.
- [48] Brunello, C. A.; Merezhko, M.; Uronen, R. L.; Huttunen, H. J. Mechanisms of secretion and spreading of pathological tau protein. *Cell Mol. Life Sci.* **2020**, *77*, 1721-1744.
- [49] Kang, C. W.; Sarnowski, M. P.; Ranatunga, S.; Wojtas, L.; Metcalf, R. S.; Guida, W. C.; Del Valle, J. R. β -Strand mimics based on tetrahydropyridazinedione (tpd) peptide stitching. *Chem. Commun.* **2015**, *51*, 16259-16262.
- [50] Gallardo, R.; Ranson, N. A.; Radford, S. E. Amyloid structures: much more than just a cross- β fold. *Curr. Opin. Struct. Biol.* **2020**, *60*, 7-16.
- [51] Li, D.; Liu, C. Hierarchical chemical determination of amyloid polymorphs in neurodegenerative disease. *Nat. Chem. Biol.* **2021**, *17*, 237-245.

Table of Contents graphic:

